Journal of Structural Geology 33 (2011) 844–858

Contents lists available at ScienceDirect

Journal of Structural Geology

journal homepage: www.elsevier.com/locate/jsg

3230–3200 Ma post-orogenic extension and mid-crustal magmatism along the southeastern margin of the Barberton Greenstone Belt, South Africa

Cristiano Lana [a,b,*], Ian Buick [c], Gary Stevens [c], Riana Rossouw [a], Willem De Wet [c]

[a] Central Analytical Facility ICP MS Unit, Department of Earth Sciences, University of Stellenbosch, Private Bag XI, Matieland 7602, South Africa
[b] Departamento de Geologia (DEGEO), Universidade Federal de Ouro Preto, Morro do Cruzeiro, Ouro preto, Minas Gerais 35400000, Brazil
[c] Department of Earth Sciences, University of Stellenbosch, Private Bag XI, Matieland 7602, South Africa

ARTICLE INFO

Article history:
Received 16 June 2010
Received in revised form
23 February 2011
Accepted 8 March 2011
Available online 15 March 2011

Keywords:
Barberton
Greenstone belt
Dome and keel
LA-ICP-MS
Geochronology

ABSTRACT

The Barberton Granitoid-Greenstone Terrain (South Africa) preserves a complex and protracted evolution involving several events of magmatism and terrain accretion along convergent tectonic boundaries. Recent studies propose that the main period of tectonic accretion and arc-related magmatism is linked to a system of divergent subduction zones above which voluminous TTG magmas were emplaced between ca. 3236 and 3227 Ma. Our structural and LA-ICP-MS U–Pb geochronology study along the southeastern margin of the Barberton Greenstone Belt (BGB) ties the waning stages of this TTG magmatism to a short (ca. <30 Ma) period of mid-crustal extension, between 3228 and 3205 Ma. We document a major NE-trending detachment that juxtaposed upper sequences (Moodies Group clastic sediments) against mid-crustal 3418 ± 10 Ma amphibolite-facies rocks of the base of the greenstone belt (Onverwacht Group rocks). Several granodiorite bodies - intruded along this detachment - contain well-preserved (syn- and post-magmatic) fabrics that are demonstrably related to extensional shearing and exhumation. Field observations and U–Pb zircon data from these granitoids are consistent with the deformation taking place at 3228 ± 10 Ma – contemporaneous with the voluminous (3236–3227 Ma) TTG magmatism in the northwestern margin of the BGB. The timing of the granodiorite emplacement also constrains a minimum age for the deposition of the Moodies Group clastic sediments, which for much of the southern and southeastern parts of the BGB must have happened before ca. 3228 Ma. 3205 ± 9 Ma subvolcanic dykes intruded into the granodiorite complex indicate that the period of exhumation and cooling of the crystalline rocks along the extensional detachment was relatively short (<30 Ma), between 3228 and 3205 Ma. Our observations combined with previously published structural data from the northwestern and southern margin of the belt suggest that the main mechanism of large-scale infolding of the supracrustal strata was shortly followed by the extension-related magmatism and subsequent, solid-state diapiric movement of the arc-related plutons.

1. Introduction

Several geochemical and structural models based on analogies with Phanerozoic and modern tectonic systems have allowed an increasing understanding of the ancient crust exposed in the Barberton Granitoid-Greenstone Terrain, South Africa (De Wit, 1982, 1983; De Wit et al., 1987; Armstrong et al., 1990; De Ronde and De Wit, 1994; Kamo and Davis, 1994; Lowe, 1994; De Ronde and Kamo, 2000; Kisters et al., 2003, 2010; Moyen et al., 2006). Structural/stratigraphic studies, in combination with U–Pb geochronology data, have identified numerous tectonostratigraphic units in the granitoid-greenstone terrain, which were juxtaposed during phases of tectonic collage and related TTG plutonism between ca. 3450 and 3100 Ma (e.g. Anhaeusser, 1969, 1984, 2001; Anhaeusser et al., 1983; Armstrong et al., 1990; De Ronde and De Wit, 1994; Kamo and Davis, 1994; Lowe, 1994; Schoene et al., 2008, 2009; Kisters et al., 2010). The Barberton Greenstone Belt (BGB) itself represents a fold-and-thrust belt that formed during two main deformation events - D1 and D2 - at ca. 3450–3440 Ma and 3230–3225 Ma respectively (e.g. De Wit et al., 1992; De Ronde and De Wit, 1994; Lowe, 1994; Lowe et al., 1999; De Ronde and Kamo, 2000). The main phase of deformation has been linked to a D2 shortening event during which much of the present-day upright NE–SW structural grain of the belt was formed (e.g. Kamo and Davis, 1994; De Ronde and De Wit, 1994; Lowe, 1994; Lana et al., 2010a,b).

* Corresponding author. Central Analytical Facility ICP MS Unit, Department of Earth Sciences, University of Stellenbosch, Private Bag XI, Matieland 7602, South Africa. Tel.: +27 21 808 4820.
E-mail address: cristianodeclana@gmail.com (C. Lana).

0191-8141/$ – see front matter © 2011 Elsevier Ltd. All rights reserved.
doi:10.1016/j.jsg.2011.03.007

Recent studies along the southern margin of the BGB associate D2 with a regional metamorphic event at ca. 3230 Ma, and subsequent exhumation of 3500–3450 Ma TTG rocks of the Southern TTG Complex (Fig. 1) (Stevens et al., 2002; Dziggel et al., 2002; Kisters et al., 2003; Diener et al., 2005; Lana et al., 2010a,b). Relatively steep foliations and down-dip lineations around the 3500–3450 Ma TTG domes have been interpreted as the result of a final diapiric movement of the seemingly hot and buoyant granitoid crust relative to the supracrustal strata (e.g., Kisters and Anhaeusser, 1995; Kisters et al., 2003; Diener et al., 2005; Van Kranendonk et al., 2009). More recently, U–Pb geochronology and structural analysis by Schoene et al. (2008, 2009) have identified major strike-slip shear zones that accommodated transcurrent movement along the southeastern and northwestern margins of the belt. In their model, Schoene et al. (2008, 2009) suggested that tectonic transpression along these marginal shear zones led to a crustal-scale, positive flower-like structural geometry for the greenstone belt (during D2) at ca. 3230–3225 Ma. However, information about the D2 transpressional features recorded in the greenstone belt strata, and details of processes that led to exhumation of the adjacent granitoid-gneiss complexes remain poorly documented.

In this study, we investigate the effects of the D2 tectonic event along the southeastern margin of the BGB based on new structural mapping and U–Pb LA-ICP-MS geochronology data. The results are used here to constrain on (1) timing of deposition of the supracrustal strata, (2) emplacement age of the adjacent granitoid complex, and (3) tectonic relationship between the imbrication/folding of greenstone strata and granitoid exhumation. We furthermore try to understand how the exhumation of the granitoid complex has influenced the present geometry and outcrop pattern of the greenstone belt.

2. Background

The Barberton Greenstone Belt (Fig. 1) is one of the oldest and best preserved Archaean greenstone belts in the world. The supracrustal strata in the main greenstone belt are commonly subdivided into three main groups - the Onverwacht, Fig Tree and Moodies Groups. The Onverwacht Group is represented by a predominantly ultramafic to mafic succession of the Lower Onverwacht Group, and felsic volcanic, volcanoclastic and sedimentary units of the Upper Onverwacht Group (Viljoen and Viljoen, 1969; Anhaeusser, 1969; Armstrong et al., 1990; Kohler and Anhaeusser, 2002; Kröner et al., 1991, 1996). Detailed stratigraphic work and U–Pb age data further subdivide the Upper Onverwacht Group into the 3474–3445 Ma Hooggenoeg Formation, 3416–3334 Ma Kromberg Formation and 3334–3298 Ma Mendon Formation (e.g., Kröner et al., 1991; Byerly et al., 1996). The Upper Onverwacht Group rocks were overlain by 3259 ± 5 to 3225 ± 3 Ma clastic and volcanoclastic (largely marine) sediments of the Fig Tree Group, and subsequently by the Moodies Group (Kröner et al., 1991; Byerly et al., 1996). The Moodies Group is an ~1–3.7 km thick sequence of arkosic, lithic and quartzose sandstones, and polymict conglomerate with siltstone, shale, jaspilite and volcanic clasts (Anhaeusser, 1976; Heubeck and Lowe, 1994). Most studies interpret the Moodies Group sequence as remnant of contractional/extensional syn-tectonic basins (see below).

Early structural and geochronological studies have identified two main tectonic events - D1 and D2 - that were associated with

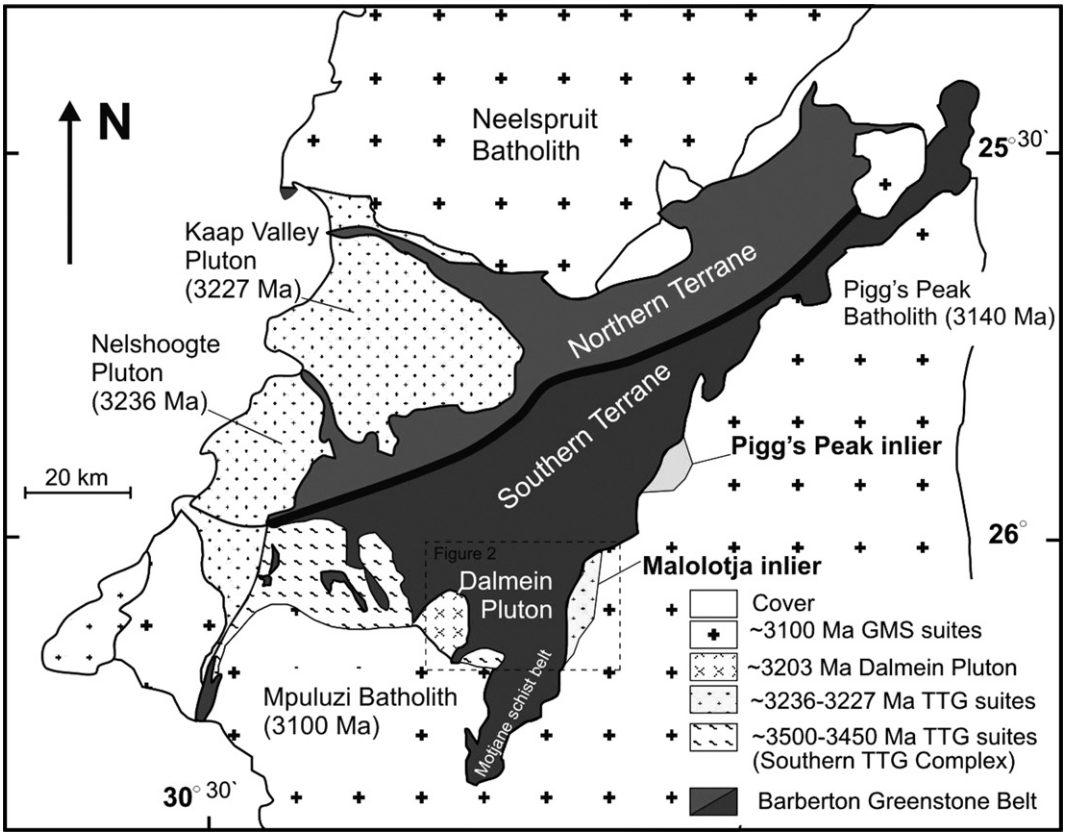

Fig. 1. Geological map of the *Barberton* Granite-Greenstone Terrain showing the *Barberton* Greenstone Belt (BGB) and surrounding granitoid batholiths and gneiss complex domes. The BGB is subdivided into two terrains: The Southern and Northern Terranes. GSM = Granite-Granodiorite-Syenite; TTG = Tonalite-Trondhjemite-Granodiorite. Boxed area shows location of Fig. 2.

episodic emplacement of tonalite-trondhjemite-granodiorite (TTG) magmas at ca. 3450–3440 and 3230–3225 Ma, roughly coinciding with the timing of deposition of the Onverwacht and Fig Tree Groups (De Wit et al., 1987, 1992; Armstrong et al., 1990; De Ronde and De Wit, 1994; Kamo and Davis, 1994; Lowe, 1994; Kröner et al., 1996). The main phase of compressional tectonics (D2) led to structural imbrications and large-scale infolding of the supracrustal strata along the present-day NE–SW trend of the belt. Most models agree that D2 involved convergence and suturing of two island arc terrains that are described as the Northern and Southern Terranes (Fig. 1) (e.g., De Ronde and De Wit, 1994; De Ronde and Kamo, 2000; Lowe and Byerly, 2007). The D2 tectonic convergence coincides with the transition from the Fig Tree Group marine sedimentation to fluvial/shallow marine (molasse-type) accumulation of the Moodies Group (Fig. 1).

Direct dating of the Moodies Group sequence across the BGB remains to be done. Nevertheless, most studies agree that for the Southern Terrain the accumulation of the sequence ended before the emplacement of the 3203 ± 7 Ma (Lana et al., 2010b) Dalmein Pluton – a kilometre-scale intrusion which sharply truncates pairs of antiforms and synforms in the southern margin of the greenstone belt (Figs. 1 and 2).

In the southeastern margin of the BGB, D2 is expressed by km-scale upright doubly plunging folds that are oriented roughly parallel to the NE–SW trend of the belt (Fig. 2; Urey, 1970). Rocks of the Onverwacht and Fig Tree Groups record an early phase of folding (D2) along a pair of NE-plunging antiform and synform structures, namely the Ngwenya synform-antiform pair (Fig. 2; Lamb, 1984). Restoration of bedding orientations indicated to Lamb (1984, 1987) that these folds were developed under horizontal shortening strain, shortly before or during the deposition of the Moodies Group. Lamb (1984) also proposed a post-Moodies Group deformation event (D3) involving reorientation of the Ngwenya structures and refolding of the greenstone sequence into an SSW-plunging synform (F3) (Figs. 2 and 3). The latter fold structure comprises the largest and easternmost SSW-plunging synform (the Malolotja synform) of the BGB, which pairs up with other km-scale folds such as the Steynsdorp and Kromberg structures (Fig. 2). The timing of D3 folding and the relationship between the fold structures and the adjacent granitoid-greenstone contact have, however, not been examined in detail.

Geochronological studies in the southeastern margin of the BGB have been focussed on two inliers of early Archaean TTG gneiss (the Pigg's Peak and Malolotja Inliers; Fig. 2) (Compston and Kröner, 1988; Kröner et al., 1989). In the Pigg's Peak Inlier, Compston and Kröner (1988) defined the earliest episode of TTG magma emplacement at 3644 ± 4 Ma, and subsequent reworking and further magmatism between ca. 3500 and 2960 Ma. U–Pb zircon data from Kröner et al. (1989) provided distinct ages of 3176 ± 8 and 3227 ± 21 Ma that were inferred as emplacement ages of tonalite magmas into ca. 3644 Ma gneisses of the so-called Ancient Gneiss Complex (AGC - Kröner et al., 1989). These authors concluded that the younger granitoid rocks (within the AGC) originated from discrete intrusions of a single magmatic event that peaked at around 3200 Ma. Based on structural analysis and ID-TIMS U–Pb zircon geochronology, Schoene et al. (2008) indicated that the amphibolite-facies gneisses of the AGC were transposed by a 1–1.5 km wide, NE-trending shear zone (the Phophonyane Shear Zone - Schoene et al., 2008) that is oriented parallel to the granitoid-greenstone belt contact. A minimum age for the shearing is given by two 3223 ± 3 Ma syntectonic granitic dykes that crosscut the mylonites but contain only a weak foliation and lineation (Schoene et al., 2008).

More recently, Schoene and Bowring (2010) have described an important suite of syntectonic magmatic rocks that are intruded near the contact with the Moodies Group, in the Malolotja Inlier (Fig. 1). These rocks record a strong magmatic fabric that progressively changes to a solid-state foliation towards the contact

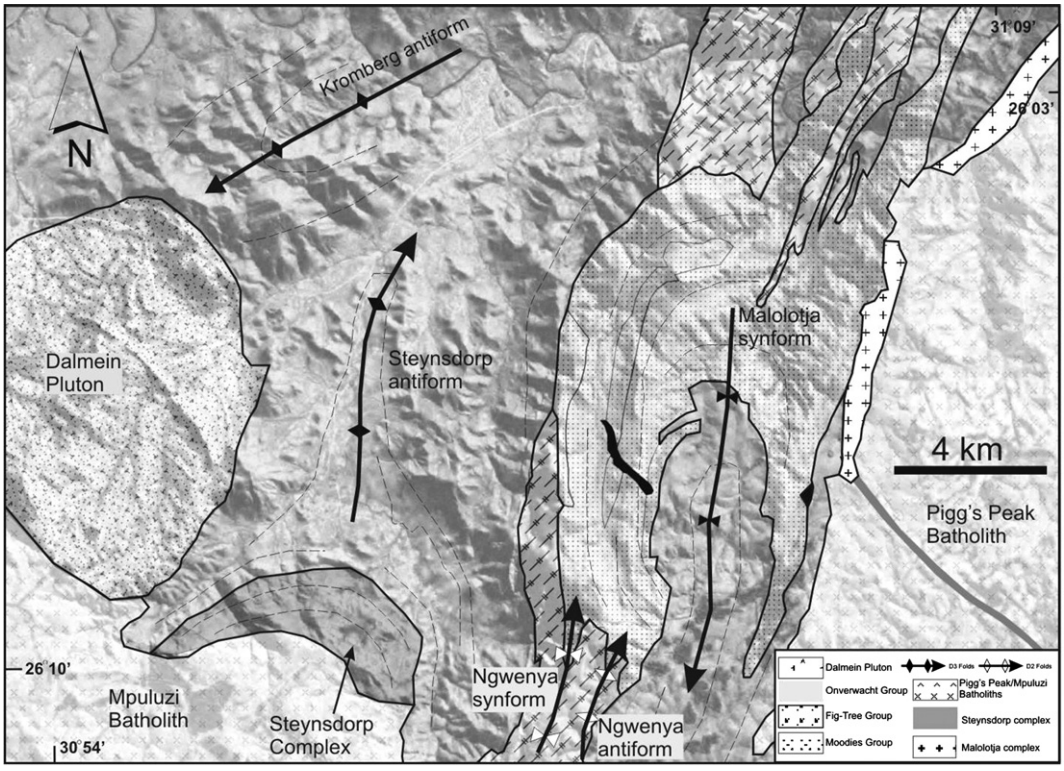

Fig. 2. Geological map of the southeastern part of the Barberton Greenstone Belt and surrounding granitoids. Map modified from Anhaeusser et al. (1984). The image in the background is an ortho-rectified LandSat image (band 1).

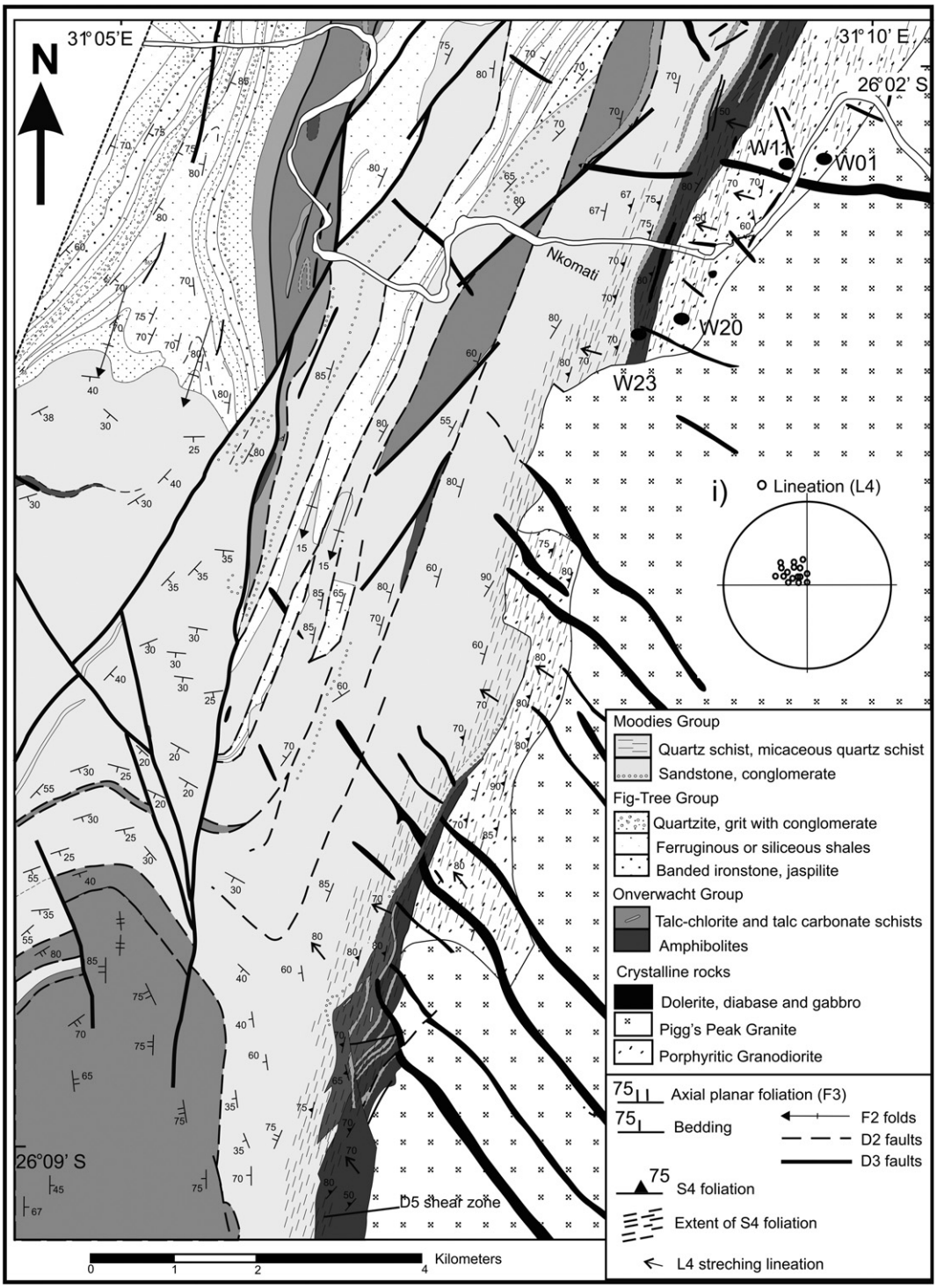

Fig. 3. Detailed structural geology map of the contact between the Malolotja synform and the granodiorite–gneiss complex. Map modified from Urey (1970). Inset (i) shows a lower hemisphere stereonet plot for L4 lineation.

with the supracrustal rocks. U–Pb ages obtained from two samples from the Malolotja Inlier suggest that magmatism and deformation occurred between 3230 ± 0.4 Ma and 3224 ± 0.5 Ma (Schoene and Bowring, 2010), overlapping in time with the shearing in the Phophonyane Shear Zone (Schoene et al., 2008). The ca. 3230–3224 Ma magmatic event was followed by emplacement of the Pigg's Peak Batholith at 3140 ± 1 Ma (Schoene and Bowring, 2007).

3. Structural Geology

3.1. The Barberton Greenstone Belt -BGB

The supracrustal strata in the southeastern part of the BGB (Fig. 1) form an 8 km wide and 20 km-long south-plunging fold structure (the Malolotja synform; Lamb, 1987), located between the Steynsdorp antiform and the Pigg's Peak Batholith (Fig. 2). The

synform is characterised by an asymmetric, W-verging geometry whereby rocks of the Onverwacht, Fig Tree and Moodies Groups dip consistently at 80°–70°W in the eastern limb and 40°–60°E in the western limb of the structure. The core of the synform folds a sharp structural unconformity that places the Onverwacht Group rocks above the Moodies Group (Lamb, 1987). This stratigraphic/structural break is described as part of a D2 frontal ramp that was folded during an E–W directed, D3 shortening event (Lamb, 1984). Similar bedding-parallel fault zones juxtapose the Moodies and Onverwacht Groups around the eastern limb of the synform (Fig. 3). These fault zones are interpreted as part of the D2 deformation structures, because they (1) truncate and deform the Moodies Group rocks (thus, post-D1) and (2) were subsequently reoriented during the D3 refolding of the supracrustal strata into the Malolotja synform (Fig. 3).

Previous regional mapping (Urey, 1970) and our structural observations indicate that the eastern limb of the Malolotja synform is sharply truncated by an NE-dipping (S4) shear zone. S4 cuts up into different stratigraphic levels of the BGB and places rocks of the Onverwacht and Moodies Groups in direct contact with the adjacent granitoid–gneiss complex of the Malolotja Inlier (Fig. 3). Regional mapping also indicates that the Fig Tree Group sequence is missing along S4, with clastic sedimentary rocks of the Moodies Group in tectonic contact with the Onverwacht Group sequence (Fig. 3). The lowermost rocks of the Onverwacht Group - located immediately above the granitoid–gneiss complex - are represented by a 20-50 m-wide sequence of amphibolite layers trending roughly NE–SW. These layers record an internal NE–SW compositional layering, which has been largely overprinted by a NE-trending foliation (S4), and subsequently intruded by a number of undeformed, fine- to medium-grained felsic dykes (Fig. 4a). S4 is a steep (70°–80°) NE–SW trending foliation, defined by biotite, hornblende and strongly recrystallized/segmented quartz-plagioclase bands (Fig. 4a). Hornblende crystals and quartz-plagioclase rods are aligned, defining a pervasive down-dip (L4) lineation that plunges consistently at 60°–70° NW (Fig. 3; inset i). Further to the west, the amphibolites intercalate with Onverwacht Group muscovite-chlorite schist, talc-chlorite schist and chert layers. These seemingly lower metamorphic grade rocks record likewise a NE-trending S4 schistosity and a prominent L4 stretching lineation that plunges 50°–60° NW (Fig. 3). L4 is defined predominantly by quartz-rods in schists and chert layers (Fig. 4b).

The Moodies Group clastic sedimentary rocks that are in direct contact with the granitoid complex or immediately above the sheared Onverwacht Group rocks were similarly overprinted during D4 (Fig. 4c, d). The sheared Moodies Group rocks are dominantly muscovite-quartz and muscovite-chlorite-quartz schists, which comprise a narrow (<200 m), but continuous D4 schist belt parallel to the granitoid-greenstone contact (Fig. 3). The schistosity is steep - 60°-80° NW-dipping - and co-planar with the S4 foliation in the amphibolite layers of the Onverwacht Group. It is, however, defined by relatively lower grade metamorphic minerals – e.g., muscovite, chlorite together with stretched quartz and feldspar. Locally, conglomeratic layers include elongated clasts of vein quartz and chert that serve as strain markers (Fig. 4d). L4 is represented by stretched quartz-feldspar aggregates or elongated conglomerate clasts that plunge predominantly 60°–70° NW. Rare macroscopic S–C fabrics and some asymmetric conglomerate clasts indicate a NW-side down/SE-side up normal sense of movement along S4.

A set of kink folds in the Moodies Group schist are also commonly observed several metres away from the amphibolites. The relationship between these kink folds and the D4 shearing is uncertain.

Fig. 4. a) Onverwacht Group amphibolites showing compositional layering and strong foliation, which were subsequently intruded by a felsic dyke. b) Strongly foliated Onverwacht chert layer, showing an NW-plunging stretching (L4) lineation. c) Strongly foliated muscovite schist of the Moodies Group along the D4 shear zone. d) Detail of the Moodies Group rocks showing stretched conglomerate clasts.

3.2. The granitoid complex

The Malolotja Inlier is located a few kilometres south of the Pigg's Peak Inlier (Fig. 1). It exposes porphyritic and medium-grained phases of a granodiorite, with a pervasive NE-trending fabric - parallel to sub-parallel to the sheared contact with the greenstone strata.This regional fabric is defined by a preferred alignment of subhedral to euhedral K-feldspar megacrysts and locally by a compositional banding (see also Schoene and Bowring, 2010). The aligned K-feldspar megacrysts may reach up to 5 cm in length and make up more than 15% of the slightly more felsic bands (Fig. 5a,b). Evidence of an igneous origin for the megacrysts includes some romb-shaped to tabular equant crystals shapes, simple twinning and zonally arranged hornblende and plagioclase inclusions (e.g., Vernon, 1986; Paterson et al., 1989, 1998). Oscillatory compositional zoning may also be observed. Plagioclase and

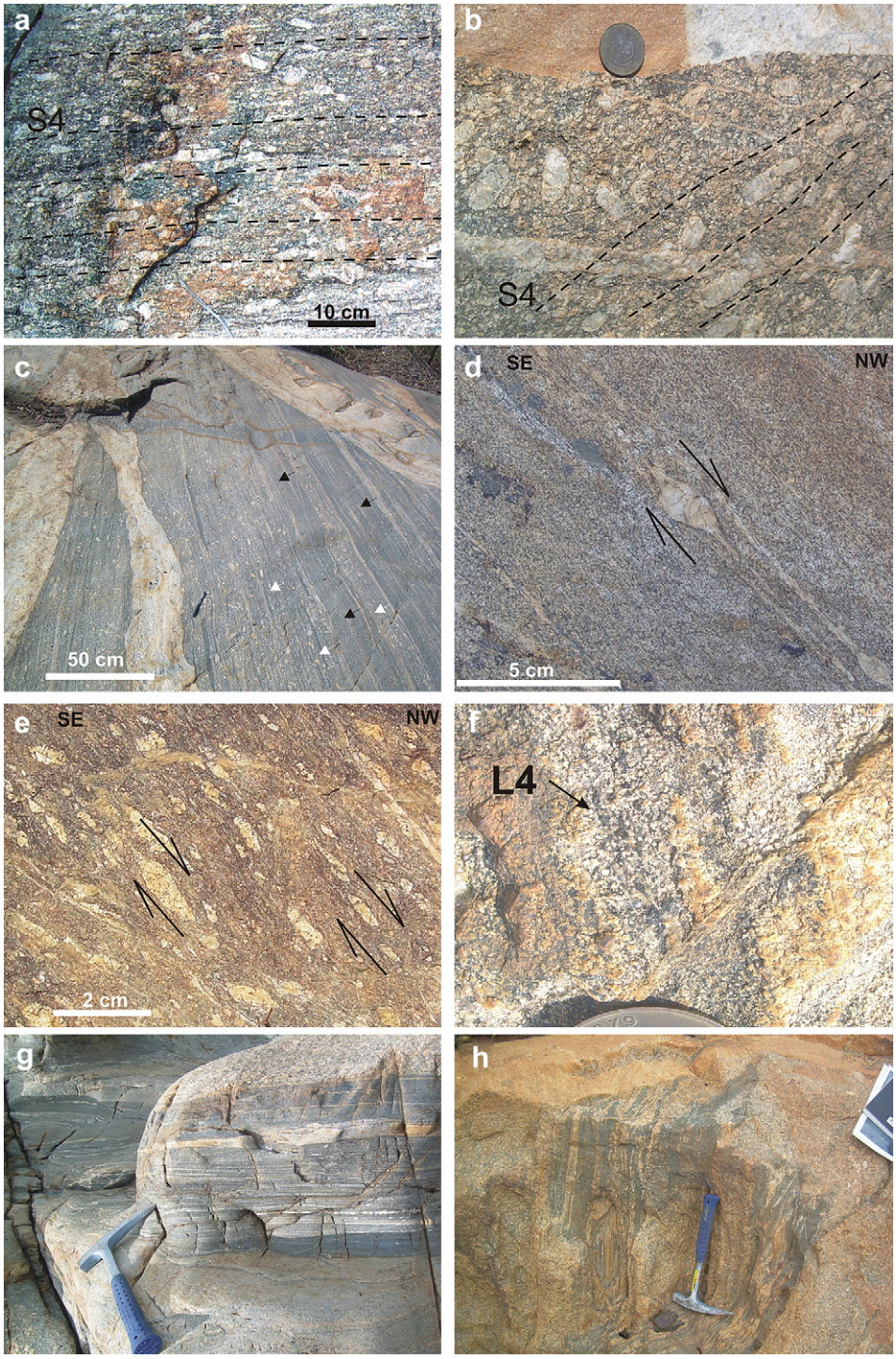

Fig. 5. a, b) Foliated granodiorite with oriented megacrysts of K-feldspar defining the main S4 fabric. c) Centimetre-wide solid-state - mylonitic - zones (black arrowheads) characterised by intense grain-size reduction due to solid-state recrystallisation of feldspars and quartz. These shear zones alternate with coarse-grained porphyritic bands (white arrowheads) of the granodiorite. d, e) Asymmetric crystals of K-feldspar indicating normal sense of shear along the D4 shear zone (plane of view SE-NW). f) L4 defined by oriented clots of hornblende. g, h) Detail of enclaves in the foliated granodiorite. The enclaves are oriented parallel to the solid-state fabric.

quartz are relatively undeformed suggesting a magmatic origin for the foliation.

The NE-trending (magmatic) foliation in the granitoid is partly transposed by a steep (70°–80°NW-dipping) mylonitic to proto-mylonitic fabric that is co-planar with the S4 foliation in the BGB (Fig. 5c,d)(see also Schoene and Bowring, 2010). There is a tendency for the solid-state fabric to become more pronounced towards the contact with the greenstone strata, but it is developed heterogeneously throughout the crystalline complex. The solid-state fabric is characterised by intense grain-size reduction - due to mineral recrystallisation - and internal compositional layering defined by alternating biotite-rich and feldspar-rich bands (Fig. 5c). Recrystallised hornblende, biotite, quartz and feldspars define the main S4 foliation. Quartz tends to be stretched and locally may form mm-long ribbons. Feldspars (K-feldspar and plagioclase) are commonly recrystallised into fine-grained aggregates. Many megacrysts have been recrystallised to augen feldspars, which vary considerably in shape, from rounded to subhedral, depending on the amount of recrystallization (Fig. 5d,e). The asymmetric geometry of many of these recrystallised megacrysts indicates a component of simple shear (Fig. 5d,e). The asymmetric megacrysts together with rare S–C fabrics consistently point to a dip-slip normal sense of shear, with the granitoid rocks (east-side) up and supracrustal strata (west-side) down.

Clots of ferromagnesian minerals (bioite-hornblende) and quartz/feldspar rods define a strong mineral lineation (Fig. 5f), oriented parallel to the L4 lineation in the sheared amphibolites, chert layers and schists in the greenstone belt. This lineation plunges 60–80° NW, consistent with the downward movement of the greenstone belt relative to the granitoid rocks.

Near the contact with the greenstone strata, the granodiorite shows several centimetre-wide rafts of amphibolite, which are interpreted as stretched mafic enclaves within the granoditorite. Additionally, the granodiorite contains metre-long/cm-wide xenoliths (or enclaves) of tonalities with a well-defined S4 mylonitic foliation (Fig. 5g,h). It is, however, uncertain whether these rocks are of the same age (same magmatic event) or represent older TTG rocks.

3.3. Crosscutting dykes

The magmatic and solid-state foliation in the granodiorite is crosscut by several centimetre- to metre-wide dykes of aphanitic to porphyritic andesite (Fig. 6a–c). The porphyritic andesite consists of medium- to coarse-grained feldspar and clinopyroxene phenocrysts embedded into a cryptocrystalline matrix. The matrix invariably shows internal flow texture defined by the alternating fine-grained and cryptocrystalline bands. A number of these dykes are intruded parallel to the main foliation in the porphyritic granodiorite, but the undeformed nature of both phenocryst minerals and matrix, indicates that the dykes themselves post-date the D4 solid-state fabric. The best exposures of these dykes were found along the Nkomati River (Fig. 3), where they range from a few millimetres to several metres in width and contain abundant host-rock inclusions and phenocrysts (Fig. 6b,c). The phenocrysts are predominantly euhedral, ranging in size from few millimetres to several centimetres (Fig. 6b,c). Poikilitic K-feldspar phenocrysts are well-zoned and contain inclusions of hornblende and quartz.

Fig. 6. a) Metre-wide dyke intrusion of aphanitic andesite into the porphyritic granodiorite. b, c) Detailed images of the andesite dyke with several cm-wide poikilitic K-feldspar crystals.

The magmatic foliation in the granodiorite is also crosscut by centimetre- to metre-wide dykes of a fine- to medium-grained granite (Fig. 5b,c). The dykes also cross cut rocks in the Onverwacht Group strata but are more common near the contact with the Pigg's Peak granite. The dykes consist dominantly of microcline, plagioclase, biotite and quartz. In places the granite dykes intrude parallel to the magmatic fabric in the granodiorite but, as with the andesite dykes, the granite dykes are undeformed, post-dating the D4 shearing in the granodiorite and Onverwacht Group strata.

3.4. Summary

Mapping in the southeastern margin of the BGB indicate the presence of ca. 300 m-wide, NW-dipping S4 normal shear zone that sharply truncates the eastern limb of the Malolotja synform - a D3 km-scale fold structure developed after the deposition of the Moodies Group sequence (Lamb, 1984). Movement along S4 juxtaposed clastic sediments of the Moodies Group and amphibolites of the Onverwacht Group against granitoid rocks of the Malolotja Inlier. The dominant granitoid in the shear zone is a porphyritic granodiorite, with minor enclaves and/or xenoliths of mafic and tonalitic compositions. This granodiorite records a regional NE-trending magmatic foliation that is gradually transposed by a parallel to sub-parallel solid-state (mylonitic) foliation towards the contact with the greenstone belt. Several andesitic dykes and medium- to coarse-grained granitic dykes, crosscut and therefore post-date the S4 fabric. These intrusives are undeformed (e.g., Figs. 5 and 6b,c) and may provide a minimum age for the deformation in the southeastern margin of the BGB.

4. Geochronology

Schoene and Bowring (2010) have provided well-constrained emplacement ages for some rocks exposed in the Malolotja Inlier. One sample of the porphyritic granodiorite (preserving primary magmatic features) has been dated at 3227–3232 Ma. A fine-grained tonalite gave a nearly identical age of ca. 3230 ± 1 Ma, whereas another sample of a granitic dyke gave an age of 3224 ± 1 Ma (Schoene and Bowring, 2010).

In the present study, we compare the age of the sheared amphibolites and granitoids with the undeformed (post-D4) intrusive dykes. Sample W23 (26° 3′ 26″ S: 31° 8′ 18″ E) represents the sheared (D4) amphibolite (e.g., Fig. 4a) of the Onverwacht Group. Sample W01 (26° 3′ 16″ S: 31° 9′ 5″ E) comes from the underlying mylonitic granodiorite of the Malolotja Inlier (Fig. 5c). Although the amphibolite and associated schists and chert layers have been previously interpreted as part of the Onverwacht Group, no previous study has provided direct age constraints for the supracrustal rocks in the southeastern margin of the BGB. Two samples from the crosscuting undeformed dykes - sample W20 (26° 3′ 53″ S: 31° 8′ 45″ E) from the fine-grained granite dyke and sample W11 (26° 3′ 21″ S: 31° 9′ 13″ E) from the andesite dyke - have also been dated to define the timing of exhumation to subsurface level (given the aphanitic texture of the crosscutting andesitic dykes; Fig. 6b,c) and a minimum age for D4 in the area.

The U–Pb zircon LA-ICP-MS analyses were carried out at the Central Analytical Facility LA-ICP-MS laboratory housed in the Department of Earth Sciences, Stellenbosch University. The analyses were performed using an Agilent 7500ce ICP-MS and a 213 nm New Wave Laser. Ablations occurred in a He carrier gas, and the resulting aerosol was mixed with Ar prior to introduction into the ICP-MS via 4 mm Tygon tubing (pre-cleaned with 1% ultra-pure nitric acid). Both unknowns and standards were ablated under identical laser conditions – e.g., 30-μm-diametre spot size, a repetition rate of 10 Hz, and an energy density of 10 J/cm^2. Concordia ages with uncertainties of approximately 1% relative (95% c.l.) were obtained from each of the secondary standards, in good agreement with their accepted TIMS ages. All U–Pb data for the unknowns (Table 1) were plotted on Wetherill concordia diagrams using the software Isoplot v.2.2 (Ludwig, 2000). Uncertainties given for individual analyses (ratios and ages) are at the 1σ level. Uncertainties in the calculated weighted mean, intercept, or concordia ages are reported at 95% confidence limits. Descriptions of instrumentation and method used for data collection can be found in the electronic supplement (ES-1).

4.1. Amphibolite (W23)

The foliated (D4) amphibolite was sampled near the contact with the porphyritic granodiorite (Fig. 3). It contains zircon grains with very complex morphologies and internal zoning. CL images of these grains show bright, structureless cores and relatively narrow (30 μm) oscillatory rims (Fig. 7). Several attempts to obtain U–Pb data from the rims resulted in highly discordant points and most likely represent U–Pb mixed ages. U–Pb data from the cores were substantially more concordant (Table 1). All points (17 points, including core and rims) plot around a poorly defined Pb-loss chord that intercepts the concordia roughly at 600 Ma and 3430 Ma (open and filled ellipses in Fig. 8a). Nine spot analyses of the cores (filled ellipses in Fig. 8a) gave a more precise upper intercept age of 3419 ± 10 Ma (MSWD = 0.34) (Fig. 8a). We interpret this 3419 ± 10 Ma upper intercept age as the best estimate of the crystallisation age for the amphibolite. Significantly, this age is identical (within error) to the 3416 ± 5 Ma age from tuff layers of the Kromberg Formation, Upper Onverwacht Group (e.g., Byerly et al., 1996). One zircon core, which is substantially brighter than the rest of the zircon separates, yielded an older concordia age of 3542 ± 13 Ma (Fig. 8a). This older core is also chemically distinct from the younger population in that it is enriched in U and Th (Table 1). This older zircon is interpreted as inherited (see discussion).

4.2. Porphyritic granodiorite (W01)

The granodiorite of the Malolotja Inlier sample W01 contains a single population of brown to pale-brown zircons that range in morphology from elongate and prismatic to relatively stubby. Most grains show rounded terminations. CL images of the grains show well-defined oscillatory zoning, surrounding CL-bright, generally structureless cores (Fig. 7). Some, but not all, oscillatory zoned overgrowths are surrounded by a thin (<2 μm) and relatively bright rim. Clear truncation of zoning between the CL-bright cores and oscillatory zoned domains has been observed on several grains. Analysis of the CL-bright cores and oscillatory zoned overgrowths revealed distinctly different $^{207}Pb/^{206}Pb$ ages. Apparent $^{207}Pb/^{206}Pb$ ages from the cores range from 3334 ± 12 to 3445 ± 14 Ma (Table 1), but the four points obtained are significantly discordant; no intercept age has been attempted. Analysis of the oscillatory zoned overgrowths yielded significantly younger $^{207}Pb/^{206}Pb$ ages. Thirteen concordant to subconcordant (>97% concordant; Table 1) points give a $^{207}Pb/^{206}Pb$ weighted mean age of 3228 ± 10 Ma (Fig. 7b). All points were considered to be representative of one $^{207}Pb/^{206}Pb$ age group, given the similar internal structure and Th/U ratios of cores and rims. The $^{207}Pb/^{206}Pb$ mean age is in good agreement with the crystallisation age of several 3227–3226 Ma trondhjemitic to granodioritic rocks observed around the margins of the greenstone belt (e.g., Kamo and Davis, 1994; Schoene et al., 2008; Lana et al., 2010b).

Table 1
LA-ICP-MS U_Pb analyses.

	[a]Th232	[a]U238	[a]Th/U	[a]Pb204	Isotopic ratios						[d]rho	Ages						Disc. %
					[b]Pb207/Pb206	[c]1σ	[b]Pb206/U238	[c]1σ	[b]Pb207/U235	[c]1σ		Pb207/Pb206	[c]1σ	Pb206/U238	[c]1σ	Pb207/U235	[c]1σ	
sample W23																		
W23-1	1344	1222	1.1	173	0.31388	0.00346	0.74414	0.00934	32.20456	0.41753	0.9681	3540	17	3586	35	3557	13	−1
W23-6	567	897	0.6	245	0.28874	0.0037	0.70119	0.00847	27.90611	0.37149	0.9074	3411	20	3425	32	3416	13	0
W23-7	767	1111	0.7	889	0.29072	0.00337	0.69328	0.00867	27.79059	0.36631	0.9488	3422	18	3395	33	3412	13	0
W23-8	232	247	0.9	132	0.2883	0.00454	0.69868	0.00945	27.77452	0.45583	0.8241	3408	24	3416	36	3411	16	0
W23-9	435	170	2.6	218	0.28849	0.00451	0.66037	0.00936	26.26472	0.44218	0.8419	3410	24	3269	36	3356	16	3
W23-10	375	122	3.1	234	0.28679	0.00545	0.62551	0.01178	24.73074	0.48657	0.9572	3400	29	3132	47	3298	19	5
W23-11	389	109	3.6	137	0.28419	0.00373	0.60549	0.00805	23.72114	0.34891	0.9039	3386	20	3052	32	3257	14	6
W23-12	121	1021	0.1	133	0.28327	0.0088	0.58449	0.01468	22.82406	0.68206	0.8405	3381	48	2967	60	3220	29	8
W23-5	234	777	0.3	448	0.27632	0.00512	0.51619	0.00928	19.66528	0.36301	0.9739	3342	29	2683	39	3075	18	13
W23-16	605	747	0.8	246	0.27335	0.00485	0.49141	0.00773	18.51979	0.3317	0.8783	3325	28	2577	33	3017	17	15
W23-17	333	1158	0.3	380	0.25749	0.00332	0.45297	0.00539	16.08131	0.21742	0.8801	3231	20	2409	24	2882	13	16
W23-18	324	955	0.3	258	0.25897	0.00596	0.42347	0.00681	15.1187	0.34578	0.7031	3241	36	2276	31	2823	22	19
W23-19	456	785	0.6	455	0.29577	0.00487	0.35625	0.00566	14.527	0.23325	0.9895	3448	25	1964	27	2785	15	29
W23-20	352	815	0.4	740	0.25032	0.00336	0.41556	0.00552	14.33676	0.21411	0.8894	3187	21	2240	25	2772	14	19
W23-21	292	1223	0.2	1018	0.25068	0.00542	0.41113	0.00629	14.20821	0.3044	0.7141	3189	34	2220	29	2764	20	20
W23-14	382	679	0.6	864	0.24557	0.00482	0.31776	0.00475	10.75114	0.21422	0.7502	3156	31	1779	23	2502	19	29
W23-15	379	980	0.4	664	0.24435	0.00694	0.20657	0.00359	6.96154	0.19045	0.6353	3149	44	1211	19	2107	24	43
sample W01																		
W01-17	88	189	0.5	568	0.25735	0.00288	0.66395	0.00769	23.55786	0.28301	0.9641	3231	18	3283	30	3250	12	−1
W01-5	345	404	0.9	891	0.25603	0.00282	0.65953	0.00771	23.28262	0.27774	0.9800	3222	17	3265	30	3239	12	−1
W01-4	250	569	0.4	1457	0.25592	0.0029	0.65485	0.00783	23.10801	0.28453	0.9711	3222	18	3247	31	3232	12	0
W01-16	271	308	0.9	805	0.25691	0.00321	0.64632	0.00817	22.8927	0.31133	0.9295	3228	20	3214	32	3222	13	0
W01-1	350	411	0.8	637	0.2563	0.0028	0.64502	0.00767	22.79439	0.27301	0.9928	3224	17	3209	30	3218	12	0
W01-18	312	594	0.5	721	0.25666	0.00358	0.64204	0.00866	22.71566	0.33906	0.9037	3226	22	3197	34	3215	15	1
W01-3	297	332	0.9	822	0.25619	0.00269	0.64278	0.00699	22.70672	0.24782	0.9964	3223	16	3200	27	3215	11	0
W01-12	17	315	0.1	645	0.25682	0.00276	0.64006	0.0076	22.66596	0.2704	0.9953	3227	17	3189	30	3213	12	1
W01-5	106	190	0.6	483	0.25898	0.00282	0.62789	0.0074	22.42198	0.26659	0.9912	3241	17	3141	29	3202	12	2
W01-14	76	271	0.3	715	0.25655	0.00294	0.62783	0.00744	22.20729	0.27473	0.9579	3226	18	3141	29	3193	12	2
W01-9	810	1292	0.6	731	0.25786	0.00279	0.61805	0.00693	21.97436	0.24974	0.9866	3234	17	3102	28	3183	11	3
W01-8	168	388	0.4	1063	0.25713	0.00285	0.61955	0.00749	21.9656	0.2683	0.9898	3229	17	3108	30	3182	12	2
W01-11	429	780	0.6	2409	0.25687	0.0027	0.61058	0.00689	21.62418	0.24353	0.9999	3228	16	3072	28	3167	11	3
W01-6	108	229	0.5	583	0.2593	0.0029	0.5716	0.00695	20.43688	0.25142	0.9883	3242	18	2914	29	3112	12	6
W01-13	348	780	0.4	282	0.26194	0.00297	0.53811	0.00632	19.43297	0.23824	0.9580	3258	18	2776	27	3064	12	9
W01-12	217	302	0.7	654	0.25581	0.00279	0.54997	0.0063	19.39699	0.22852	0.9723	3221	17	2825	26	3062	11	8
W01-4	233	565	0.4	868	0.25805	0.00276	0.53167	0.00591	18.91612	0.2108	0.9975	3235	17	2749	25	3038	11	10
W01-17	42	69	0.6	133	0.2438	0.00267	0.52188	0.00604	17.54271	0.20363	0.9971	3145	17	2707	26	2965	11	9
W01-10	87	244	0.4	589	0.26299	0.00283	0.46803	0.00535	16.97179	0.19435	0.9982	3265	17	2475	23	2933	11	16
W01-10	92	339	0.3	647	0.26158	0.00283	0.46548	0.00529	16.78764	0.19491	0.9788	3256	17	2464	23	2923	11	16
W01-11	335	335	1.0	700	0.22936	0.00296	0.32087	0.00404	10.14516	0.14023	0.9109	3048	21	1794	20	2448	13	27
W01-3	659	1067	0.6	1977	0.25777	0.00274	0.47156	0.00539	16.76	0.19253	0.9950	3233	17	2490	24	2921	11	15
W01-26	596	615	0.5	1210	0.29348	0.00686	0.10717	0.003	4.33096	0.17395	0.6807	3436	36	656	17	1699	33	61
W01-28	712	605	0.5	1110	0.27676	0.002535	0.32446	0.004	12.38153	0.2326	0.6579	3345	14	1812	20	2634	18	31
W01-2	826	134	0.3	465	0.27499	0.00285	0.36809	0.005	13.97143	0.27555	0.6295	3335	16	2020	22	2748	19	26
W01-24	1068	806	0.7	1114	0.27483	0.002035	0.23019	0.003	8.72164	0.12951	0.8338	3334	12	1336	15	2309	14	42
sample W11																		
W011-28	386	420	0.9	590	0.25486	0.00301	0.60515	0.00715	21.26354	0.26805	0.9373	3215	19	3051	29	3151	12	3
W011-1	141	284	0.5	742	0.25552	0.00438	0.62026	0.00806	21.84665	0.36241	0.7833	3219	27	3111	32	3177	16	2
W011-3	177	355	0.5	989	0.24851	0.00493	0.64283	0.00888	22.03873	0.42482	0.7166	3175	31	3200	35	3185	19	0
W011 -4	171	523	0.3	1118	0.25382	0.00522	0.6311	0.00862	22.07527	0.45171	0.6675	3209	32	3154	34	3187	20	1
W011-5	104	389	0.3	1056	0.2538	0.00515	0.63091	0.00806	22.07564	0.46441	0.6073	3209	32	3153	32	3187	20	1
W011-6	302	266	1.1	764	0.25098	0.00534	0.63969	0.00877	22.1318	0.50033	0.6064	3191	33	3188	34	3190	22	0
W011-7	273	272	1.0	810	0.2536	0.00553	0.63387	0.00843	22.16133	0.49805	0.5918	3207	34	3165	33	3191	22	1
W011-8	150	378	0.4	1049	0.25524	0.00389	0.6321	0.00735	22.24317	0.33583	0.7702	3218	24	3158	29	3194	15	1

W011-9	69	146	0.5	401	0.25325	0.00498	0.63682	0.00778	22.24483	0.42711	0.6363	3205	31	3177	31	3195	19	1
W011-10	79	167	0.5	489	0.25281	0.00555	0.63909	0.00828	22.27918	0.50372	0.5730	3203	34	3185	33	3196	22	0
W011-11	169	197	0.9	514	0.24907	0.00401	0.65199	0.00747	22.4171	0.35635	0.7207	3179	25	3236	29	3202	15	−1
W011-12	88	261	0.3	706	0.25186	0.00368	0.64959	0.00963	22.55574	0.37699	0.8870	3197	23	3227	38	3208	16	−1
W011-13	80	336	0.2	762	0.25556	0.00323	0.64185	0.00689	22.61569	0.2751	0.8825	3220	20	3196	27	3211	12	0
W011-14	105	207	0.5	564	0.25597	0.00323	0.64326	0.0073	22.70207	0.28332	0.9093	3222	20	3202	29	3214	12	0
W011-2	495	372	1.3	1070	0.25334	0.0033	0.65329	0.00801	22.81623	0.3084	0.9071	3206	20	3241	31	3219	13	−1
W011-15	139	398	0.3	1098	0.25481	0.00378	0.6516	0.00762	22.91207	0.34475	0.7772	3215	23	3235	30	3223	15	0
sample W20																		
W-20-3	535	1342	0.4	285	0.24233	0.00311	0.62452	0.00833	20.86761	0.29634	0.9392	3135	20	3128	33	3133	14	0
W-20-4	555	908	0.6	207	0.24384	0.0028	0.6206	0.00702	20.86358	0.24894	0.9480	3145	18	3112	28	3132	12	1
W-20-5	565	999	0.6	429	0.24385	0.00275	0.61869	0.00696	20.80199	0.24593	0.9515	3145	18	3105	28	3129	11	1
W-20-6	1068	1111	1.0	734	0.24266	0.00269	0.62678	0.00743	20.97084	0.25606	0.9708	3138	18	3137	29	3137	12	0
W-20-7	155	769	0.2	510	0.24383	0.00275	0.61872	0.00694	20.80138	0.24568	0.9497	3145	18	3105	28	3129	11	1
W-20-8	95	647	0.1	733	0.24317	0.00284	0.61763	0.00707	20.70621	0.251	0.9443	3141	18	3101	28	3125	12	1
W-20-9	137	957	0.1	332	0.24442	0.00296	0.60908	0.00765	20.5293	0.27649	0.9326	3149	19	3066	31	3117	13	2
W-20-10	170	435	0.4	218	0.24339	0.00308	0.61113	0.00806	20.50371	0.2867	0.9432	3142	20	3075	32	3115	14	1
W-20-11	327	935	0.3	474	0.2438	0.00303	0.60484	0.00784	20.32808	0.279	0.9444	3145	20	3049	32	3107	13	2
W-20-12	307	875	0.4	807	0.24436	0.00314	0.60285	0.00712	20.30942	0.26344	0.9105	3149	20	3041	29	3106	13	2
W-20-13	271	872	0.3	357	0.24365	0.00324	0.60383	0.00813	20.27992	0.29462	0.9268	3144	21	3045	33	3105	14	2
W-20-14	465	678	0.7	218	0.24369	0.00405	0.59617	0.00855	20.03024	0.35303	0.8137	3144	26	3014	35	3093	17	3
W-20-16	114	909	0.1	807	0.24541	0.00327	0.56186	0.00744	19.01115	0.26337	0.9558	3155	21	2874	31	3042	13	6
W-20-17	188	800	0.2	234	0.2454	0.00434	0.54147	0.00776	18.32135	0.33429	0.7855	3155	28	2790	32	3007	18	7
W-20-18	866	789	1.1	137	0.24755	0.00314	0.52248	0.0067	17.81728	0.24809	0.9210	3169	20	2710	28	2980	13	9
W-20-21	356	547	0.7	740	0.24772	0.0026	0.41891	0.00485	14.30769	0.16639	0.9956	3170	17	2256	22	2770	11	19
W-20-22	565	908	0.6	1018	0.24645	0.00299	0.41914	0.00523	14.24074	0.19208	0.9251	3162	19	2257	24	2766	13	18
W-20-23	324	888	0.4	664	0.24931	0.00276	0.39365	0.00468	13.53249	0.16705	0.9631	3180	17	2140	22	2718	12	21
W-20-24	796	867	0.9	474	0.24527	0.00275	0.37158	0.0045	12.56564	0.15565	0.9777	3155	18	2037	21	2648	12	23
W-20-25	908	897	1.0	1234	0.24741	0.00304	0.32758	0.00404	11.1753	0.15091	0.9133	3168	19	1827	20	2538	13	28

[a] U and Pb concentrations and Th/U ratios are calculated relative to GJ-1 reference zircon.
[b] Corrected for background and within-run Pb/U fractionation and normalised to reference zircon GJ-1 (ID-TIMS values/measured value); $^{207}Pb/^{235}U$ calculated using $(^{207}Pb/^{206}Pb)/(^{238}U/^{206}Pb * 1/137.88)$.
[c] Quadratic addition of within-run errors and daily reproducibility of GJ-1.
[d] Error correlation defined as the quotient of the propagated errors of the $^{206}Pb/^{238}U$ and the $^{207}Pb/^{235}U$ ratio.

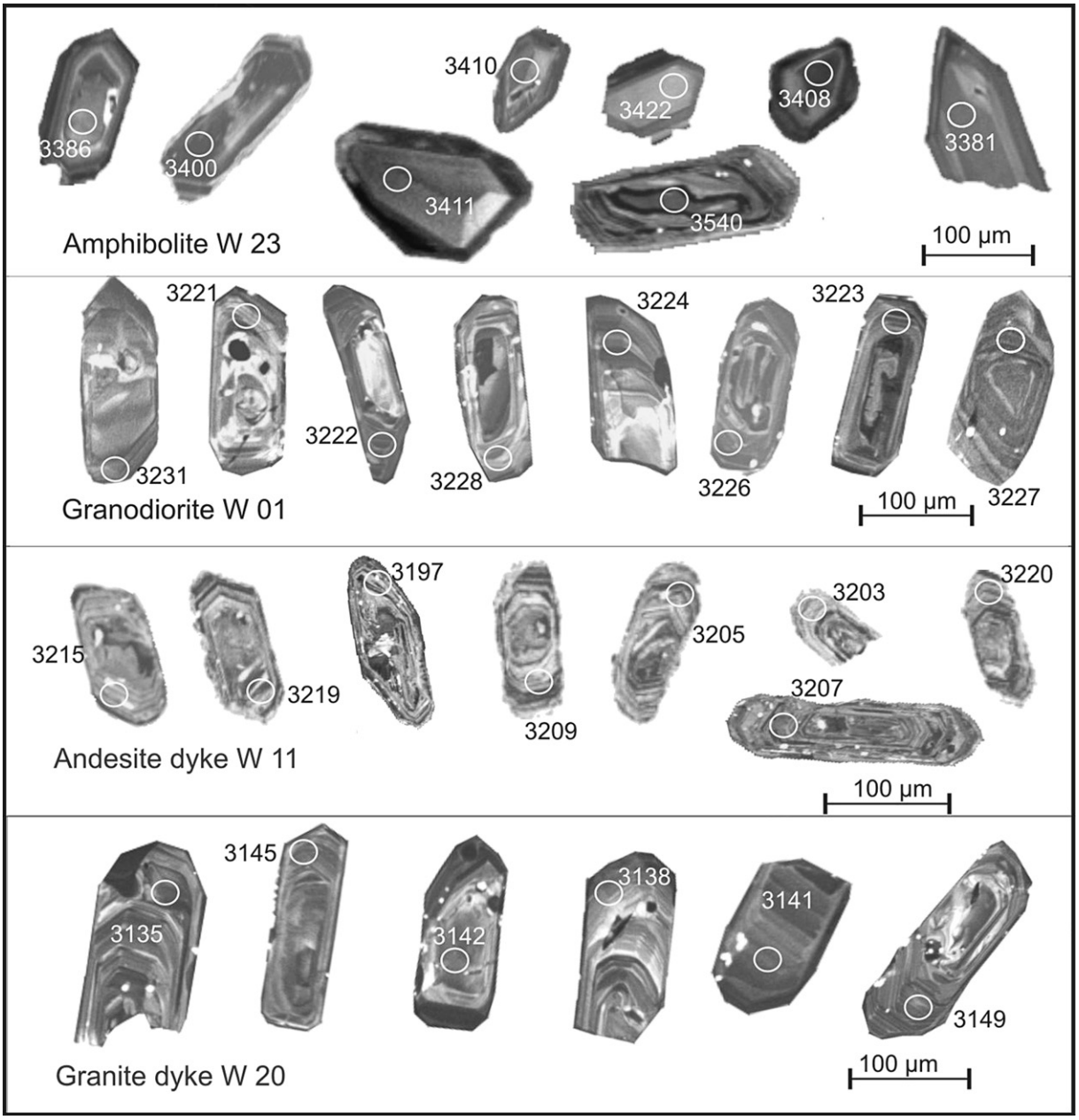

Fig. 7. Zircon CL images for samples of the sheared amphibolite (W23), granodiorite (W01), andesite dyke (W11) and granite dyke (W20).

4.3. Subvolcanic andesite (W11)

The andesite dyke contains colourless to pale-brown fractured zircons, which vary from equant to elongate prisms, with well-defined faces and round terminations (Fig. 7). Cathodoluminescence imaging shows strongly zoned magmatic rims surrounding bright structureless centres (Fig. 7). Thin (<2 um) bright outer overgrowths are also visible in some grains. Sharp truncations between bright cores and magmatic zoning were, however, not clear for most grains. Analysis on the oscillatory rims and bright centres of these grains gave concordant to subconcordant points with a $^{206}Pb/^{207}Pb$ weighted mean age of 3208 ± 12 Ma (Table 1). Fifteen of these points gave a more precise concordia age of 3205 ± 9 Ma (MSWD of concordance and equivalence = 1.2) (Fig. 8c). We interpret the concordia age as the best estimation of the crystallisation age of the subvolcanic andesite.

4.4. Granite dyke (W20)

The sample from the undeformed granite dyke, which crosscuts the S4 in the granodiorite, contains relatively large (>100 um) zircons that are translucent, ranging in colour from yellow to pale-brown. Most grains are fractured and contain abundant mineral inclusions. The grains are internally complex with either CL-bright or -dark cores that are surrounded by oscillatory zoned magmatic domains (Fig. 7). The absence of unambiguous truncation between the cores and oscillatory zoning suggests that these internal structures are co-magmatic. Twenty two analyses of the cores and the oscillatory zoned overgrowths scatter along recent Pb-loss discordia segment that intercepts the upper concordia at 3143 ± 4 Ma (MSWD = 2.4). An identical (albeit less precise) $^{206}Pb/^{207}Pb$ weighted mean age of 3143 ± 11 Ma (95% confidence) is given by the concordant to subconcordant data (12 point >97%

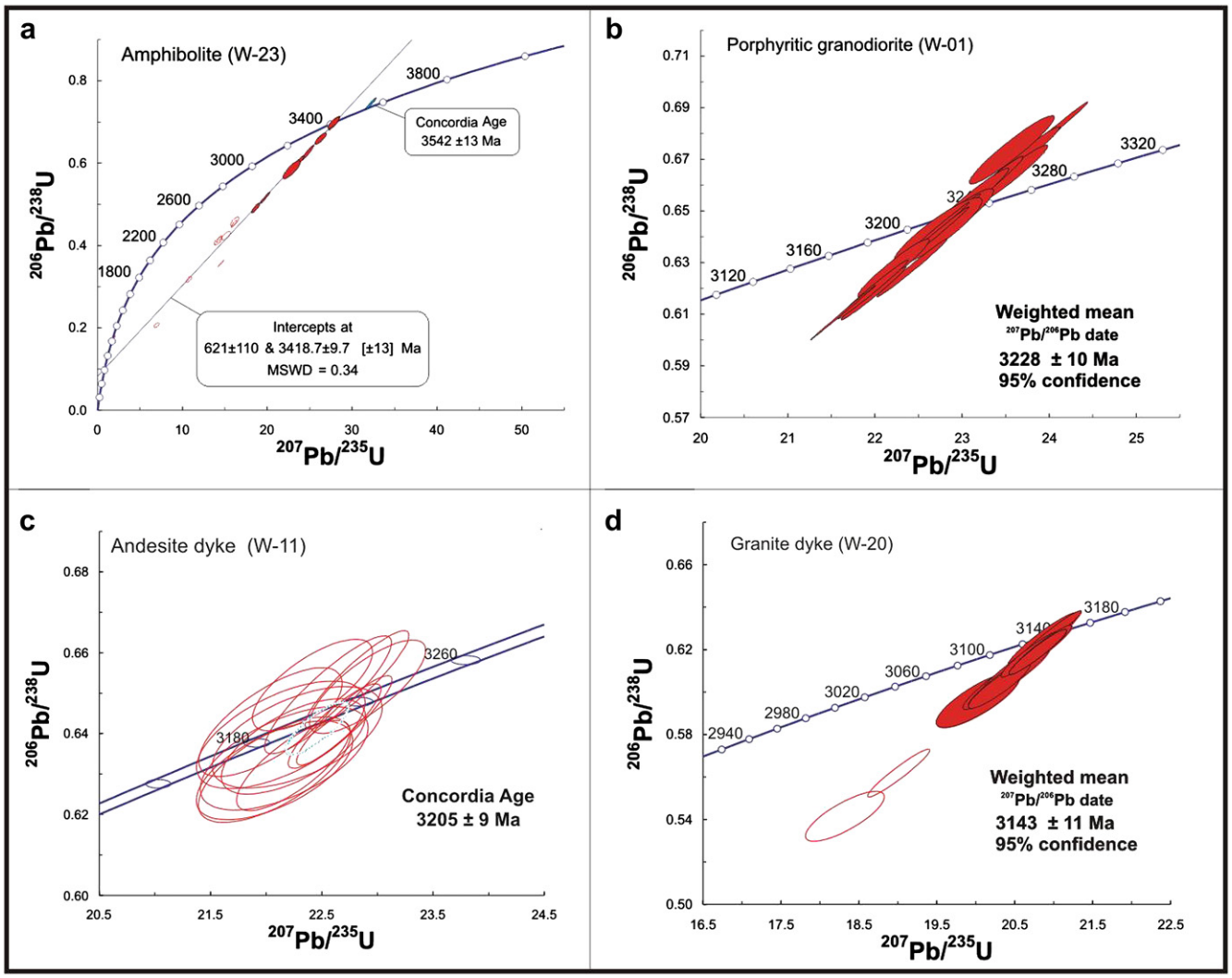

Fig. 8. U–Pb concordia diagram plots for the (a) Onverwacht amphibolites (W23), (b) granodiorite (W01), (c) andesite dyke (W11) and (d) granite dyke (W20).

concordant; Fig. 8d). Both ages are identical within error to the 3140 ± 1 Ma TIMS age obtained from a sample of the Pigg's Peak Batholith, located a few kilometres to the north of our study area (Schoene and Bowring, 2007).

5. Discussion

5.1. D4 extension in the eastern margin of the BGB

The granite-greenstone contact along the eastern margin of the BGB is defined by a highly tectonized and lithologically heterogeneous, NW-dipping (S4) shear zone that separates the amphibolite-facies granitoid complex of the Malolotja Inlier from the greenstone belt strata. To the west of the contact, rocks the greenstone belt record earlier phases of deformation (D2 and D3; Lamb, 1984) that led to formation of a series of roughly upright (doubly plunging) pairs of synforms and antiforms. Our structural mapping indicates that the eastern limb of the main F3 fold structure - the Malolotja synform – is sharply truncated by S4 (Fig. 3). S4 juxtaposes rocks of the Moodies and Onverwacht Groups against granitoids of the Maloloja Inlier (Fig. 3).

Results of U–Pb ICP-MS (W23; Fig. 8a) indicate that the lowermost unit of the Onverwacht strata overprinted by S4 (the amphibolite layers) crystallised at 3418 ± 10 Ma, coinciding in time with the extrusion of the 3416 ± 5 Ma tuff layers of the Kromberg Formation (e.g., Kröner et al., 1991; Byerly et al., 1996). We suggest that the amphibolites (as well as the overlying talc and chlorite schists and chert layers) represent buried volcanics and volcanoclastic rocks of the Upper Onverwacht Group. The 3542 ± 13 Ma inherited zircon core in the amphibolite (Fig. 7a) indicate the presence of a 3500–3550 Ma basement, equivalent to gneiss complexes exposed in the southern and eastern margins of the greenstone belt - e.g., Steynsdorp Complex or Ancient Gneiss Complex (e.g., Kröner et al., 1996; Lana et al., 2010a).

The foliated porphyritic granodiorite in the footwall of the shear zone has aligned euhedral K-feldspar megacrysts and biotite clots (e.g., Fig. 5a,b) that are oriented parallel to the NE-trending contact with the BGB (see also Schoene and Bowring, 2010). This magmatic foliation has been documented from several granodiorite plutons in central Swaziland and in the Southern TTG complex (Fig. 1), and it probably represents a regional NE-trending magmatic fabric (Schoene and Bowring, 2010; Lana et al., 2010b). The megacrystic fabric is, however, gradually transposed into a solid-state, protomylonitic, and ultimately mylonitic NE-trending fabric, towards the granitoid-greenstone contact (Fig. 5c). Kinematic indicators and down-dip lineations recorded along the mylonitic foliation indicate

a progressive exhumation of the granodiorite relative to the Moodies Group sequence. Significantly, structural elements recorded along the shear zone and stratigraphic relationships between Moodies and Onverwacht Group rocks (e.g., disappearance of Fig Tree Group strata) are all consistent with a normal geometry for the shear zone, and characterise D4 as an extensional event.

The progressive overprinting from the NE-trending magmatic foliation by the NE-trending solid-state foliation towards the contact with the greenstone belt strata suggests that magmatism and extension were likely synchronous events. This is true given the fact that the foliations are co-planar (NE-trending) and that both fabrics are aligned parallel to the main NE-trend of the greenstone belt. One sample of the sheared granodiorite (W01; Fig. 8b) - collected a few metres from the granitoid-greenstone contact – yielded U–Pb age of 3228 ± 10 Ma, which is within error of the ages obtained for other porphyritic granodiorites in central Swaziland (Schoene and Bowring, 2010) and in the Southern TTG complex (Lana et al., 2010b). The crystallisation age of the granodiorite also overlaps within error with the main period (3230-3226 Ma) of exhumation of the TTG complexes in the southern margin of the BGB (e.g., Kisters et al., 2003; Diener et al., 2005; Lana et al., 2010b). We suggest that the D4 shearing in the eastern margin of the greenstone belt is directly related to the regional (post-orogenic) extension and core complex formation in the southern margins of the BGB (e.g., Kisters et al., 2003; Diener et al., 2005).

The S4 fabric in the granodiorite is crosscut by the andesite dyke, for which we have obtained a U–Pb Concordia age of 3205 ± 9 Ma (Fig. 8c). These dykes are characterised by a fine-grained to aphanitic matrix and romb-shaped feldspar phophyrocrystals (Fig. 6b,c), representing the first dated subvolcanic material that crosscuts crystalline granitoid-gneisses around the BGB. The U–Pb data and crosscutting relationships between S4 and the andesite dykes clearly indicate that granodiorite was exhumed to shallow crustal levels before ca. 3205 Ma.

5.2. Timing constraints on the Moodies group deposition

Important stratigraphic breaks within the BGB, including the sharp transition from marine sedimentation of the Fig Tree Group to intramontane/foreland clastic sedimentation of the Moodies group have been linked to the main D2 phase of tectonism and tectonic collision in the Barberton Terrain (see reviews by Lowe and Byerly, 2007). Geochronological work in the central and southern parts of the greenstone belt suggests that this transition occurred sometime between 3230 and 3225 Ma, with the end of the Fig Tree volcanic activity at 3225 ± 3 Ma (Byerly et al., 1996). In the southeastern margin of the BGB, Lamb (1984) suggested that the deposition of the Moodies Group marks a period of intense E-W shortening and folding of the supracrustal strata during D2 and D3. In this context, the timing of deformation of the Moodies Group sequence has become of particular interest because these clastic sediments are interpreted as part of syn- to post-collisional basins, accumulated after the deposition of the 3225 Ma Fig Tree volcanics (e.g., Kroner et al., 1991). Yet, the entire Moodies Group was largely folded between 3236 and 3227 Ma granitoid domes around the southern and northwestern margins of the greenstone belt (Fig. 1) (e.g., De Ronde and De Wit, 1983; Heubek and Lowe, 1994; Lowe et al., 1999).

Our structural observations and U–Pb data indicate that the D3 folding of the Moodies Group into the Malolotja synform was followed by the D4 extension and exhumation of the granitoid complex between 3228 ± 10 and 3205 ± 9 Ma. More importantly, the timing for the D4 extensional shearing at 3228 ± 10 Ma requires that the deposition and concomitant D3 folding of the Moodies Group occurred during the final stages of the Fig Tree Group deposition, overlapping in time with the extrusion of the 3225 ± 3 Ma felsic volcanics in the central part of the BGB (e.g., Kroner et al., 1991; Byerly et al., 1996). Similar field constraints have been documented in the southern margin of the greenstone belt, where the timing for the deposition and infolding of the Moodies Group is bracketed between the 3225 Ma Fig Tree Group felsic rocks and the emplacement of the 3226 ± 9 Ma porphyritic granotids (Figs. 1 and 2) (Lana et al., 2010b). The D3 shortening of the greenstone sequence was thus a relatively short lived event, followed by D4 extension and exhumation of the granitoid complexes in the southeastern and southern margins of the BGB.

5.3. Implications for the post-collisional history of the BGB

Several workers have attempted to incorporate the large-scale infolding of greenstone belts and vertical exhumation of granitoid rocks into tectonic scenarios involving crustal inversion, extensional collapse or regional transpression (e.g., Anhaeusser, 1984; Hippertt, 1994; Alkimim and Marshak, 1998; Kisters et al., 2003; Van Kranendonk et al., 2004; Lana et al., 2010a, b). The vertical movement between greenstone belt strata and surrounding granitoids - which define the main dome and keel geometry of Archaean greenstone terrains - has been recorded in Barberton (South Africa), Quadrilatero Ferrifero (Brazil) and in the Pilbara and Yilgarn Cratons (Australia) (e.g., Alkimim and Marshak, 1998; Kisters et al., 2003; Van Kranendonk et al., 2004; Weinberg and van der Borgh, 2008).

In the Australian examples, the normal shear zones at granite-greenstone contacts are generally circular with radial, down-dip lineations around the domal granitic bodies. The supracrustal rocks record a coherent upward-younging stratigraphy, which precludes significant thrusting prior to exhumation of the granitoids (e.g., Van Kranendonk et al., 2004). In the Barberton terrain this structural pattern for granitoids and supracrustal rocks is not often observed. In addition to wide-spread evidence for overthrusting and thickening of the greenstone belt (Lamb, 1984, 1987; Lowe et al., 1999), many granitoid areas such as the Steyndorp dome and the Malolotja and Pigg's Peak inliers record a dominant unidirectional pattern for the mineral stretching lineation (Lana et al., 2009; Schoene et al., 2009; this study).

Models by De Ronde and De Wit (1994) and De Ronde and Kamo (2000) propose that thrusting and duplication of the Barberton supracrustal strata occurred during the D2 terrain accretion, followed by a period of transition to strike-slip/transtensional tectonics at circa 3100 Ma. Based on thermochronology data and structural observations, Schoene et al. (2008, 2009) proposed a period (>100 Ma) of transform boundary tectonics, which led to large-scale juxtaposition of middle to lower crustal basement orthogneiss complexes against upper crustal greenstone sequences. In the Pigg's Peak Inlier (Fig. 1), Schoene et al. (2008) documented gently (<20°NE) plunging stretching lineations along a NE-trending amphibolite-facies shear zone (the Phophonyane Shear Zone). Rare asymmetric feldspars crystals within the shear zones and small displacements in crosscutting dykes indicate a dominant strike-slip component during shearing (Schoene et al., 2008). More recently, Schoene and Bowring (2010) have linked this strike-slip shearing to compressional strains derived from convergence and accretion of the BGB strata onto an >3500 Ma older cratonic block of the Ancient Gneiss terrain. In this model, the granodiorites emplaced in the Malolotja Inlier have been interpreted as part of a much broader arc-related magmatic suite (the 3236–3220 Ma Usutu suite) observed in central Swaziland (Schoene and Bowring, 2010).

Our geochronological data and textural observations are in good agreement with the previous suggestions that the 3228 ± 10 Ma

porphyritic granodiorite - in the Malolotja Inlier - is part of the extensive, ca. 3230 Ma arc-related Usutu suite (Schoene and Bowring, 2010). Similar ca. 3227 Ma porphyritic granodiorites are also commonly observed in the southern margin of the BGB: some of which record syn-magmatic mylonitic shear zones that accommodated the exhumation of the Southern TTG complex (Lana et al., 2010b) and are likely to be part of the Usutu suite documented by Schoene and Bowring (2010).

However, the structures recorded in the porphyritic granodiorite and adjacent greenstone strata in the study area do not support models involving large strike-slip displacements in the eastern margin of the greenstone belt. The pervasive unidirectional, down-dip mineral lineation (L4) and asymmetric structural elements recorded in the study area are rather consistent with normal (dip-slip) movement along the D4 shear zone. More importantly, the normal sense of shear recorded in the 3228 ± 10 Ma porphyritic granodiorite (e.g., Fig. 5d–f) suggests extension instead of regional transpression. The steep fabrics and down-dip lineations reflect the relative upward movement of the 3500 Ma old crystalline block in the western margin of the BGB, which was most likely exhumed during collapse of the 3236–3220 Ma Usutu magmatic arc. The final stages of this exhumation is punctuated by the intrusion of the subvolcanic andesite dyke at ca. 3205 ± 9 Ma, suggesting a short lived (<30 Ma) extensional event.

Evidence for pervasive down-dip mineral lineations and greenstone strata-down/granitoids-up sense of shear are not only limited to the Malolotja Inlier, but have been well documented around the margins of the Nelsoogte and Kaap Valley granitoids as well as in the adjacent Nelsoogte and Stolzburg schist belts (Anhaeusser, 1984, 2001; Kisters et al., 2003). The 3227 Ga Kaap Valley and 3236 Ma Nelshoogte Plutons were exhumed shortly after emplacement in the northwestern margin of the greenstone belt, in the very same manner to the emplacement of the granitoids in the Malolotja Inlier (see Anhaeusser, 2001; Kisters et al., 2003 for details). In addition, the 3228 Ma age for the extension in the eastern margin of the BGB suggested here coincides in time with the 3230–3227 Ma magmatism and exhumation of the Southern TTG complex (Kisters et al., 2003; Lana et al., 2010b). Thus, in contrast to the recent transpressional model by Schoene et al. (2008), we propose that much of the eastern and western margins of the BGB record a syn- to post-Moodies shortening deformation that is related to the effects of vertical movements of the 3236 ± 1 Ma Nelsoogte, 3227 ± 1 Ma Kaap Valley and 3228 ± 10 Ma Malolotja granitoids. The granitoid emplacement and solid-state shearing (D4) in the Malolotja Inlier were contemporaneous with the solid-state exhumation of high-P-low-T granitoids of the southern margin of the greenstone belt (Lana et al., 2010b).

Acknowledgements

We would like to acknowledge support from Lutz Nasdla, Jiri Slama and Elena Belousova who kindly provided important standards for our LA-ICP-MS laboratory. We also thank technical advice provided by Craig Storey and Marc Poujol, and comments from Keith Benn on an earlier version of the manuscript. Constructive comments by Roberto Weinberg, Carl Anhaeusser and Associate Editor João Hippertt were gratefully appreciated.

Appendix. Supplementary data

Supplementary data related to this article can be found online at doi:10.1016/j.jsg.2011.03.007.

References

Alkimim, F.F., Marshak, S., 1998. Transamazonian orogeny in the southern Sao Francisco craton region, Minas Gerais, Brazil: evidence for Paleoproterozoic collision and collapse in the Quadrilatero Ferrıfero. Precambrian Research 90, 29–58.

Anhaeusser, C.R., 1969. The Stratigraphy, Structure and Gold Mineralization of the Jamestown and Sheba Hills Area of the Barberton Mountain Land. Ph.D. Thesis. University of the Witwatersrand, Johannesburg, South Africa, 322 p.

Anhaeusser, C.R., 1976. The geology of the Sheba Hills area of the Barberton mountain land, South Africa, with particular reference to the Eureka Syncline. Transactions of the Geological Society of South Africa 79, 253–280.

Anhaeusser, C.R., 1984. Structural elements of Archaean granite–greenstone terranes as exemplified by the Barberton mountain land, South Africa. In: Kroener, A., Greiling, R. (Eds.), Precambrian Tectonics Illustrated. E. Schweizerbartsche Verlagsbuchhandlung, Stuttgart, Germany, p. 419.

Anhaeusser, C.R., 2001. The anatomy of an extrusive-intrusive Archaean mafic-ultramafic sequence: the Nelshoogte schist belt and Stolzburg Layered ultramafic complex, Barberton greenstone belt, South Africa. South African Journal of Geology 104, 167–204.

Anhaeusser, C.R., Robb, L.J., Viljoen, M.J., 1983. Notes on the provisional geological map of the Barberton greenstone belt and surrounding granitic terrane, eastern Transvaal and Swaziland (1:250,000 colour map). In: Anhaeusser, C.R. (Ed.), Contributions to the Geology of the Barberton Mountain Land. Geological Society of South Africa Special Publications, vol. 9, pp. 221–223.

Armstrong, R.A., Compston, W., De Wit, M.J., Williams, I.S., 1990. The stratigraphy of the 3.5–3.2 Ga Barberton greenstone belt revisited: a single zircon ion microprobe study. Earth and Planetary Sciences Letters 101, 90–106.

Byerly, G.R., Kröner, A., Lowe, D.R., Todt, W., Walsh, M.M., 1996. Prolonged magmatism and time constraints for sediment deposition in the early Archaean Barberton greenstone belt: evidence from the Upper Onverwacht and fig tree groups. Precambrian Research 78, 125–138.

Compston, W., Kröner, A., 1988. Multiple zircon growth within early Archaean tonalitic gneiss from the Ancient Gneiss Complex, Swaziland. Earth Planetary Science Letters 87, 13–28. doi:10.1016/0012-821X(88)90061-1.

De Ronde, C.E.J., Kamo, S., 2000. An Archaean arc-arc collisional event: a short-lived (ca. 3 Myr) episode, Weltevreden area, Barberton greenstone belt, South Africa. Journal of African Earth Sciences 30, 219–248.

De Ronde, C.E.J., De Wit, M.J., 1994. Tectonic history of the Barberton greenstone belt, South Africa: 490 million years of Archaean crustal evolution. Tectonics 13, 983–1015.

De Wit, M.J., Armstrong, R.A., Hart, R.J., Wilson, A.H., 1987. Felsic igneous rocks within the 3.3 to 3.5 Ga Barberton greenstone belt: high crustal level equivalents of the surrounding tonalite–trondhjemite terrain emplaced during thrusting. Tectonics 6, 529–549.

De Wit, M.J., Roering, C., Hart, R.J., Armstrong, R.A., De Ronde, C.E.J., Green, R.W.E., Tredoux, M., Peberdy, E., Hart, R.A., 1992. Formation of an Archaean continent. Nature 357, 553–562.

Diener, J.F.A., Stevens, G., Kisters, A.F.M., Poujol, M., 2005. Metamorphism and exhumation of the basal parts of the Barberton greenstone belt, South Africa: constraining the rates of Mesoarchaean tectonism. Precambrian Research 143, 87–112.

Dziggel, A., Stevens, G., Poujol, M., Anhaeusser, C.R., Armstrong, R.A., 2002. Metamorphism of the granite-greenstone terrane south of the Barberton greenstone belt, South Africa: an insight into the tectono–thermal evolution of the lower portions of the Onverwacht Group. Precambrian Research 114, 221–247.

Heubeck, C., Lowe, D.R., 1994. Late syndepositional deformation and detachment tectonics in the Barberton greenstone belt, South Africa. Tectonics 13, 1514–1536.

Hippertt, J.F.M., 1994. Structures indicative of helicoidal flow in a migmatitic diaper (Bacao Complex, southeastern Brazil). Tectonophysics 234, 169–196.

Kamo, S.L., Davis, D.W., 1994. Reassessment of Archaean crustal development in the Barberton mountain land, South Africa, based on U–Pb dating. Tectonics 13, 167–192.

Kisters, A.F.M., Anhaeusser, C.R., 1995. Emplacement features of Archaean TTG plutons along the southern margin of the Barberton greenstone belt, South Africa. Precambrian Research 75, 1–15.

Kisters, A.F.M., Stevens, G., Dziggel, A., Armstrong, R.A., 2003. Extensional detachment faulting at the base of the Barberton greenstone belt: evidence for a 3.2 Ga orogenic collapse. Precambrian Research 127, 355–378.

Kisters, A.F.M., Belcher, G., Dziggel, A., Poujol, M., 2010. Continental growth and convergence-related arc plutonism in the Mesoarchaean: evidence from the Barberton granitoid-greenstone terrain, South Africa. Precambrian Research 178, 15–26.

Kohler, E., Anhaeusser, C.R., 2002. Geology and geodynamic setting of Archaean silicic metavolcaniclastic rocks of the Bien venue formation, fig tree group, northeast Barberton greenstone belt, South Africa. Precambrian Research 116, 199–235.

Kröner, A., Compston, W., William, I.S., 1989. Growth of early Archaean crust in the Ancient Gneiss Complex of Swaziland as revealed by single zircon dating. Tectonophysics 161, 271–298.

Kröner, A., Byerly, G.R., Lowe, D.R., 1991. Chronology of early Archaean granite-greenstone evolution in the Barberton mountain land, South Africa, based on precise dating by single zircon evaporation. Earth Planetary Sciences Letters 103, 41–54.

Kröner, A., Hegner, E., Wendt, J.I., Byerly, G.R., 1996. The oldest part of the Barberton granitoid-greenstone terrain, South Africa, evidence for crust formation between 3.5 and 3.7 Ga. Precambrian Research 78, 105–124.

Lamb, S.H., 1984. Structures on the eastern margin of the Archaean Barberton greenstonebelt, northwest Swaziland. In: Kröner, A., Greiling, R. (Eds.), Precambrian Tectonics Illustrated. Verlag E. Schweizerbart, Stuttgart, pp. 19–40.

Lamb, S.H., 1987. Archaean synsedimentary tectonic deformation- a comparison with the Quaternary. Geology 15, 565–568.

Lana, C., Kisters, A., Stevens, G., 2010a. Exhumation of MesoArchaean TTG gneisses from the middle crust: insights from the Steynsdorp core complex, Barberton granitoid-greenstone terrain, South Africa. Geological Society of America Bulletin 122, 183–197.

Lana, C., Tohver, E., Cawood, P., 2010b. Quantifying rates of dome-and-keel formation in the Barberton granitoid-greenstone belt, South Africa. Precambrian Research 177, 199–211.

Lowe, D.R., 1994. Accretionary history of the Archaean Barberton greenstone belt (3.55–3.22 Ga), southern Africa. Geology 22, 1099–1102.

Lowe, D.R., Byerly, G.R., 2007. An overview of the geology of the Barberton greenstone belt: implications for early crustal development. In: van Kranendonk, M.J., et al. (Eds.), Developments in Precambrian Geology, vol. 15, pp. 481–526.

Lowe, D.R., Byerly, G.R., Heubeck, C., 1999. Structural divisions and development of the west-central part of the Barberton greenstone belt. In: Lowe, D.R., Byerly, G.R. (Eds.), Geologic Evolution of the Barberton Greenstone Belt, South Africa. Geological Society of America Special Paper, vol. 329, pp. 83–114.

Ludwig, K.R., 2000. Isoplot/Ex: a Geochronological Toolkit for Microsoft Excel. Berkeley, California. In: Berkeley Geochronology Center Special Publication, vol. 1a 53 p.

Moyen, J.F., Stevens, G., Kisters, A.F.M., 2006. Record of mid-Archaean subduction from metamorphism in the Barberton terrain of South Africa. Nature 442, 559–562.

Paterson, S.R., Vernon, R.H., Tobisch, O.T., 1989. A review of criteria for the identification of magmatic and tectonic foliations in granitoids. Journal of Structural Geology 11, 349–363.

Paterson, S.R., Fowler, T.K.J., Schmidt, K.L., Yoshinobu, A.S., Yuan, E.S., Miller, R.B., 1998. Interpreting magmatic fabric patterns in plutons. Lithos 44, 53–82.

Schoene, B., Bowring, S.A., 2007. Determining accurate temperature-time paths from U–Pb thermochronology: an example from the SE Kaapvaal Craton, Southern Africa. Geochimica et Cosmochimica Acta 71, 165–185.

Schoene, B., Bowring, S.A., 2010. Rates and Mechanisms of MesoArchaean Magmatic Arc Construction, Eastern Kaapvaal Craton. In: Geological Society of America Bulletin, vol. 122 408–429.

Schoene, B., De Wit, M.J., Bowring, S.A., 2008. MesoArchaean assembly and stabilization of the eastern Kaapvaal craton. A structural-thermochronological perspective. Tectonics 27, 1–27.

Schoene, B., Duda, F.O., De Wit, M.J., Bowring, S.A., 2009. Sm–Nd isotopic mapping of lithospheric growth and stabilization in the eastern Kaapvaal craton. Terra Nova 21, 219–228.

Stevens, G., Droop, G.T.R., Armstrong, R.A., Anhaeusser, C.R., 2002. Amphibolite facies metamorphism in the Schapenburg schist belt: a record of the mid-crustal response to 3.23 Ga terrane accretion in the Barberton greenstone belt. South African Journal of Geology 105, 271–284.

Urey, 1970. Geological Map of Swaziland (1:250,000 Colour Map). Geological survey and mines department, Mbabane, Swaziland.

Van Kranendonk, M.J., Collins, W.J., Hickman, A.H., Pawley, M.J., 2004. Critical tests of vertical vs horizontal tectonic models for the Archaean east Pilbara granite-greenstone terrane, Pilbara craton, western Australia. Precambrian Research 131, 173–211.

Van Kranendonk, M.J., Kröner, A., Connelly, J., 2009. Age, lithology and structural evolution of the c. 3.53 Ga Theespruit Formation in the Tjakastad area, southwestern Barberton greenstone belt, South Africa, with implications for Archaean tectonics. Chemical Geology 261, 115–139.

Vernon, R.H., 1986. K-feldspar megacrysts in granites — phenocrysts, not porphyroblasts. Earth-Science Reviews 23, 1–63.

Viljoen, M.J., Viljoen, R.P., 1969. An Introduction to the Geology of the Barberton Granite-Greenstone Terrain. In: Special Publication of the Geological Society of South Africa, vol. 2 9–28.

Weinberg, R.F., van der Borgh, P., 2008. Extension in the Archean Kalgoorlie terrane, Yilgarn craton. Precambrian Research 161, 77–88.

De Wit, M.J., 1982. Gliding and overthrust nappe tectonics in the Barberton greenstone belt. Journal of Structural Geology 4, 117–136.

De Wit, M.J., 1983. Notes on a preliminary 1:25,000 geological map of the southern part of the Barberton greenstone belt. In: Anhaeusser, C.R. (Ed.), Contributions to the Geology of the Barberton Mountain Land. Geological Society of South Africa Special Publication, vol. 9, pp. 185–187.